TISSUE ENGINEERING: Part A
Volume 20, Numbers 7 and 8, 2014

DOI: 10.1089/ten.tea.2013.0386

Three-Dimensional Printed Multiphase Scaffolds for Regeneration of Periodontium Complex

Chang H. Lee, PhD, Jeffrey Hajibandeh, DDS, Takahiro Suzuki, DDS, PhD, Andrew Fan, Peng Shang, PhD, and Jeremy J. Mao, DDS, PhD

Tooth-supporting periodontium forms a complex with multiple tissues, including cementum, periodontal ligament (PDL), and alveolar bone. In this study, we developed multiphase region-specific microscaffolds with spatiotemporal delivery of bioactive cues for integrated periodontium regeneration. Polycarprolactione-hydroxylapatite (90:10 wt%) scaffolds were fabricated using three-dimensional printing seamlessly in three phases: 100-μm microchannels in Phase A designed for cementum/dentin interface, 600-μm microchannels in Phase B designed for the PDL, and 300-μm microchannels in Phase C designed for alveolar bone. Recombinant human amelogenin, connective tissue growth factor, and bone morphogenetic protein-2 were spatially delivered and time-released in Phases A, B, and C, respectively. Upon 4-week *in vitro* incubation separately with dental pulp stem/progenitor cells (DPSCs), PDL stem/progenitor cells (PDLSCs), or alveolar bone stem/progenitor cells (ABSCs), distinctive tissue phenotypes were formed with collagen I-rich fibers especially by PDLSCs and mineralized tissues by DPSCs, PDLSCs, and ABSCs. DPSC-seeded multiphase scaffolds upon *in vivo* implantation yielded aligned PDL-like collagen fibers that inserted into bone sialoprotein-positive bone-like tissue and putative cementum matrix protein 1-positive/dentin sialophosphoprotein-positive dentin/cementum tissues. These findings illustrate a strategy for the regeneration of multiphase periodontal tissues by spatiotemporal delivery of multiple proteins. A single stem/progenitor cell population appears to differentiate into putative dentin/cementum, PDL, and alveolar bone complex by scaffold's biophysical properties and spatially released bioactive cues.

Introduction

A TOOTH IS A COMPLEX ORGAN consisting of hard and soft tissues, including enamel, dentin, cementum, and vascularized dental pulp. The periodontium refers to tissues surrounding and supporting the tooth, including cementum, periodontal ligament (PDL), and alveolar bone. Despite textbook definition as separate anatomical entities, tooth root and the periodontium is functionally a single unit.[1–3] Approximately 64% of the U.S. population has lost at least one permanent tooth due to dental caries, periodontal disease, trauma, or genetic disorders.[4–7] The field of tooth regeneration has grown robustly.[8–20] The ambitious goal to regenerate an entire tooth, including the enamel, has encountered several barriers, such as the unavailability of patient compatible, postnatal stem/progenitor cells, and lack of strategy to derive functional ameloblasts.[12] A less ambitious and pragmatic goal to regenerate mineralized tooth roots has gained substantial momentum.[9,17,19] Dentin-like and cementum/PDL-like tissues were formed *in vivo* from dental pulp stem/progenitor cells (DPSCs) and PDL stem/progenitor cells (PDLSCs), respectively.[11,21] A tooth root-like structure with PDL-like tissue was formed in hydroxyapatite (HA)/tricalcium phosphate cylinder that was loaded with stem cells from apical papilla and PDLSCs.[17] PDL cells were seeded on bioengineered dentin surface to simulate cementum–PDL complex *in vitro*.[2] Delivery of two growth factors, Stromal cell-derived factor 1 and bone morphogenetic protein-7 (BMP7), induced mineralized tissue formation along with a PDL-like structure in alveolar bone sockets following tooth extraction in the rat.[9] Transplantation of allogeneic dental mesenchymal stem/progenitor cells in HA scaffold in extraction socket supported the function of a prosthetic crown.[19] Despite the progress in tooth root regeneration, an existing barrier is to regenerate not only multiple tissues of an anatomically correct tooth root but also the supporting PDL and alveolar bone in one integrated strategy and by using the patient's endogenous cells.[22]

Biophysical properties of scaffolds, such as surface tomography, internal microstructure, scale and interconnectivity of pores/channels, and material elasticity, play important roles in cell adhesion, migration, proliferation, and differentiation.[22–28]

Center for Craniofacial Regeneration (CCR), Columbia University Medical Center, New York, New York.

Apatite microtopography with 10–400 μm pores significantly promoted PDL reattachment to root and alveolar bone by PDLSCs in comparison with smooth dentin surface and nanostructured HA.[22] Nanohybrid matrix scaffolds with microtubular structure were fabricated to mimic dentinal tubules.[29] Polycaprolactone (PCL) fibers with perpendicularly oriented microchannels improved collagen attachment in mineralized structures.[26] These emerging findings suggest that biophysical properties of material scaffolds may impact on tooth root and/or periodontium regeneration. However, little is known what design and biophysical parameters are pivotal for the regeneration of periodontium complex.

In this report, we created a region-specific scaffold with three phases of microstructures, preoptimized for the regeneration of dentin/cementum, PDL, and alveolar bone from dental stem/progenitor cells. Three-dimensional (3D) layer-by-layer fabrication enables precise control of the scaffold's microarchitecture in different regions, in conjunction with spatiotemporal delivery of amelogenin as a stimulant for mineralized dentin/cememtum formation,[30] connective tissue growth factor (CTGF) as per our previous work to stimulate bone marrow stromal/stem cells toward fibroblasts[31] for PDL regeneration, and BMP2 as an osteoinductive agent[32] to stimulate alveolar bone regeneration. These three recombinant human proteins were microencapsulated in poly(lactic-co-glycolic acid) (PLGA) microspheres (μS) and time-released in Phases A, B, and C with different pore/channel scales of an integrated multiphase PCL/HA scaffold. *In vitro* and *in vivo* data collectively demonstrated that dental stem/progenitor cells were stimulated by spatiotemporally delivered bioactive cues and produced type I collagen (COL-I) fibers that inserted into dentin sialophosphoprotein-positive ($DSPP^+$)/cementum matrix protein 1-positive ($CEMP1^+$) mineralized matrix on one side and bone sialoprotein-positive (BSP^+) bone-like tissue on another side, which together recapitulated a putative periodontium complex.

Materials and Methods

Fabrication of multiphase scaffolds with spatiotemporal delivery of bioactive cues

PCL/HA scaffolds were fabricated ($5\times5\times3\,mm^3$) by layer-by-layer deposition using 3D printing (Bioplotter; EnvisionTec) as per our previous work.[33,34] Briefly, PCL and HA (90:10 wt%) was comolten at 120°C and dispensed through a 28-gauge metal needle (DL Technology) to create interlaid strands (diameter 100 μm) and interconnected microchannels (Fig. 1). To construct integrated multiphase microstructures, dispensing parameters including distance in

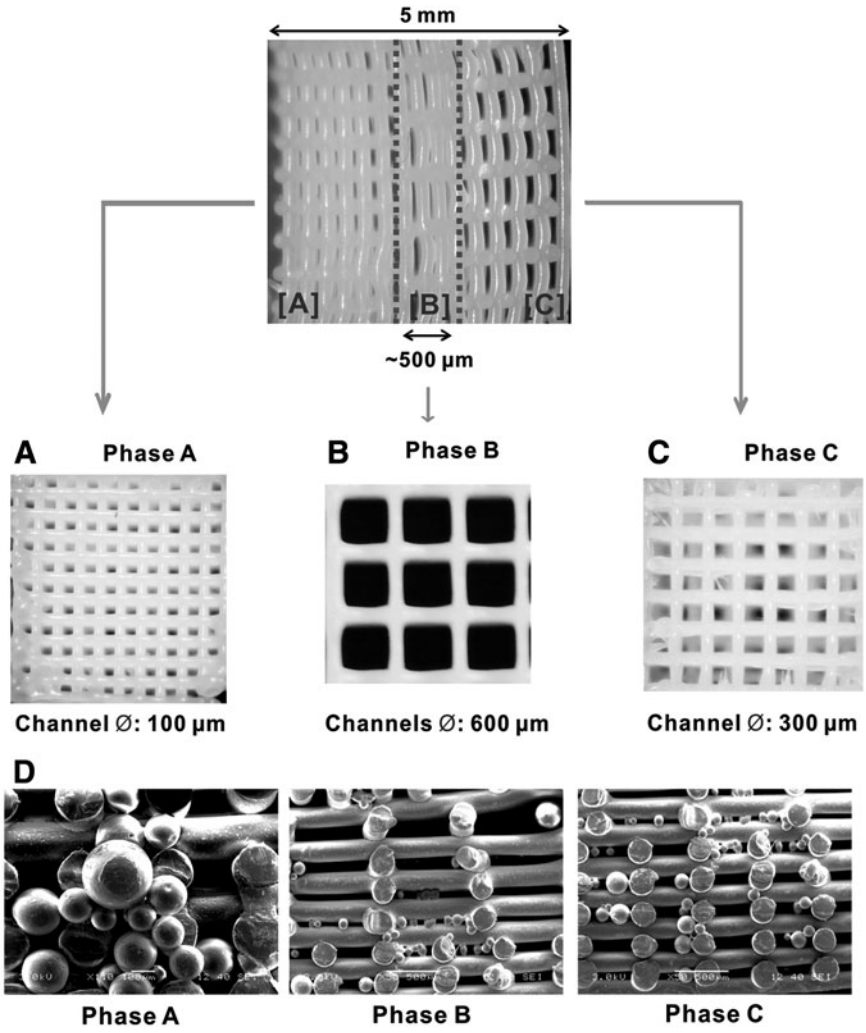

FIG. 1. Three-dimensional (3D) printed seamless scaffold with region-specific microstructure and spatial delivery of proteins. The fabricated scaffolds consisted of three phases: 100-μm microchannels with 2.5 mm in width **(A;** Phase A), 600-μm microchannels with 500 μm in width **(B;** Phase B), 300-μm microchannels with 2.25 mm in width **(C;** Phase C). **(D)** Poly(lactic-co-glycolic acid) microspheres encapsulating amelogenin, connective tissue growth factor (CTGF), and bone morphogenetic protein-2 (BMP2) were spatially tethered to Phases A, B and C, respectively.

between interlaid microstrands were varied. The fabricated scaffold consisted of three phases: (A) 100-μm transverse microchannels with 2.25 mm in width designed for cementum/dentin interface, (B) 600-μm transverse microchannels with 0.5 mm in width designed for the PDL, and (C) 300-μm transverse microchannels with 2.25 mm in width designed for alveolar bone (Fig. 1A–C). These design parameters were selected with reference to microscopic scales in the literature[35] and also our prior experience in the regeneration fibro-osseous tissues.[31,36]

To direct cell differentiation, PLGA μS encapsulating recombinant human amelogenin, CTGF, and BMP2 were incorporated in Phases A, B, and C of the scaffold, respectively (Fig. 1D). Amelogenin is a secreted protein by ameloblasts and participates in mineralization.[37] CTGF was selected for its potency to stimulate fibroblastic differentiation.[31,38] BMP2 was selected for its ability to promote osteogenesis.[32] Natively, amelogenin is expressed by ameloblasts and was selected to simulate odontogenesis and/or cementogenesis, its effect to promote differentiation of odotoblasts and cementoblasts.[30,39,40] Consistently, our pilot study showed that amelogenin promote DPSC's differentiation into odontoblast-like cells (data not shown). PLGA μS-encapsulating these bioactive cues were prepared using double-emulsion technique as per our previous work.[31,38] *In vitro* release kinetics showed timed extrusion of the encapsulated cues up to the tested 6 weeks (Supplementary Fig. S1; Supplementary Data are available online at www.liebertpub.com/tea). Then, a total of 10-mg PLGA μS encapsulating recombinant human amelogenin (10 μg), CTGF (5 μg), or BMP2 (2.5 μg) were suspended in 1 mL ethanol, air-dried 1 h for ethanol evaporation, and then delivered into the scaffold's microchannels in Phases A, B, and C, respectively. As described in our previous work,[31] μS-suspended in ethanol with preoptimized volume was pipetted through microchannels in each phase of scaffold to achieve phase-specific μS incorporation. Scaffold's microstructures and μS incorporation were imaged with scanning electronic microscopy (S-4700; Hitachi High Technologies). The PLGA μS-incorporated scaffolds were sterilized in ethylene oxide (ETO) for 24 h before cell seeding. Our previous work showed minimal loss of protein potency following ETO sterilization in comparison to other methods.[31,36] Identical scaffolds with empty PLGA μS (no proteins) were used as controls for *in vitro* and *in vivo* experiments.

For dentin/cementum formation, a pilot study was conducted to obtain optimal size and/or pattern of microchannels that promote the differentiation of dental stem/progenitor cells into odontoblasts and/or cementoblasts (Supplementary Fig. S2). Our data showed that 100-μm channels in 3D-printed scaffolds are superior in promoting odontoblastic differentiation than other channel sizes tested (Supplementary Fig. S2).

Cell preparation and delivery

Following IRB approval, human DPSCs, PDLSCs, and alveolar bone stem/progenitor cells (ABSCs) were isolated from 18- to 39-year-old patients as per our previous methods.[41–43] Briefly, tooth pulp and PDL samples were minced and digested with collagenase (3 mg/mL) and dispase (4 mg/mL) for 1 h at 37°C for DPSC and PDLSC isolation, respectively. Mononucleated and adherent cells were isolated by single-cell suspension and passage through a 70-mm strainer (BD). The isolated cells were cultured in DMEM supplemented with 10% fetal bovine serum (Atlanta Biological) and 1% antibiotics at 37°C and 5% CO_2 with the medium change twice a week. To isolate ABSCs, alveolar bone samples were cultured to allow the migration of mononucleated and adherent cells out of bone marrow. Previously, we isolated, expanded, and differentiated DPSCs, PDLSCs, and ABSCs into osteo-/odontoblasitc, chondrogenic, and adipogenic lineages.[41–45]

Passage 2–4 DPSCs, PDLSCs, or ABSCs were suspended at a density of 1×10^5 cells/scaffold in a neutralized COL-I solution (2 mg/mL). Cell-suspended collagen solution was then infused into scaffold's microchannels and incubated for 1 h at 37°C. Cell-seeded multiphase scaffolds were cultured in 12-well plates for 2 days before *in vivo* implantation or cultured for 4 weeks *in vitro* in chemically defined media, a 1:1 mixture of osteo-/odontogenic supplements and fibroblastic differentiation supplements as per our previous methods.[31,34,46] Total 10 samples per group were cultured for *in vivo* experiments.

In vivo *implantation of cell-delivered scaffolds*

Under IACUC approval, 10-week-old immunodeficient mice (Harlan) were anesthetized with 1–5% isofluorane. Upon disinfection with 10% povidone iodine and 70% ethanol, a 15-mm incision was made in the dorsum's midsagittal plane. Following creation of subcutaneous pouches, DPSC-seeded multiphase scaffolds with spatiotemporal delivery of BMP2, CTGF, and amelogenin were implanted, followed by wound closure ($n = 10$). DPSC-seeded scaffolds with empty μS were implanted as control ($n = 10$). The rationale for delivery of DPSCs, as opposed to PDLSCs or ABSCs, in the present *in vivo* experiment is that DPSCs have been more thoroughly characterized[41–45] and are readily available in extracted teeth that are currently discarded as medical waste. Following 6-week *in vivo* implantation, all constructs were retrieved from mice following euthanasia by CO_2 inhalation.

Gene expression

Total RNA was isolated from each phase of the cultured scaffolds using Trizol as per our previous work.[31,34,46] All isolated RNA samples were reverse-transcribed using a kit (Applied Biosystems). For mRNA quantification, real-time quantitative polymerase chain reaction (PCR) with the cDNA samples were performed using ViiA™ 7 Real-Time PCR System and TaqMan® gene expression assays (Applied Biosystems). Commercially available primers and probes for human COL-I, CEMP1, DSPP, and BSP were used with GAPDH as a housekeeping gene.

Histomorphometric and immunohistochemical analyses

The harvested samples were embedded in paraffin and sectioned at 5 μm thickness. Randomly selected sections were stained with H&E, Masson's Trichrome, and Alizarin Red (AR) as per our previous work.[31,33,34] Immunofluorescence for COL-I (ab90395; Abcam), DSPP (ab122321), CEMP1 (ab134231), and BSP (ab52128) was performed as per our

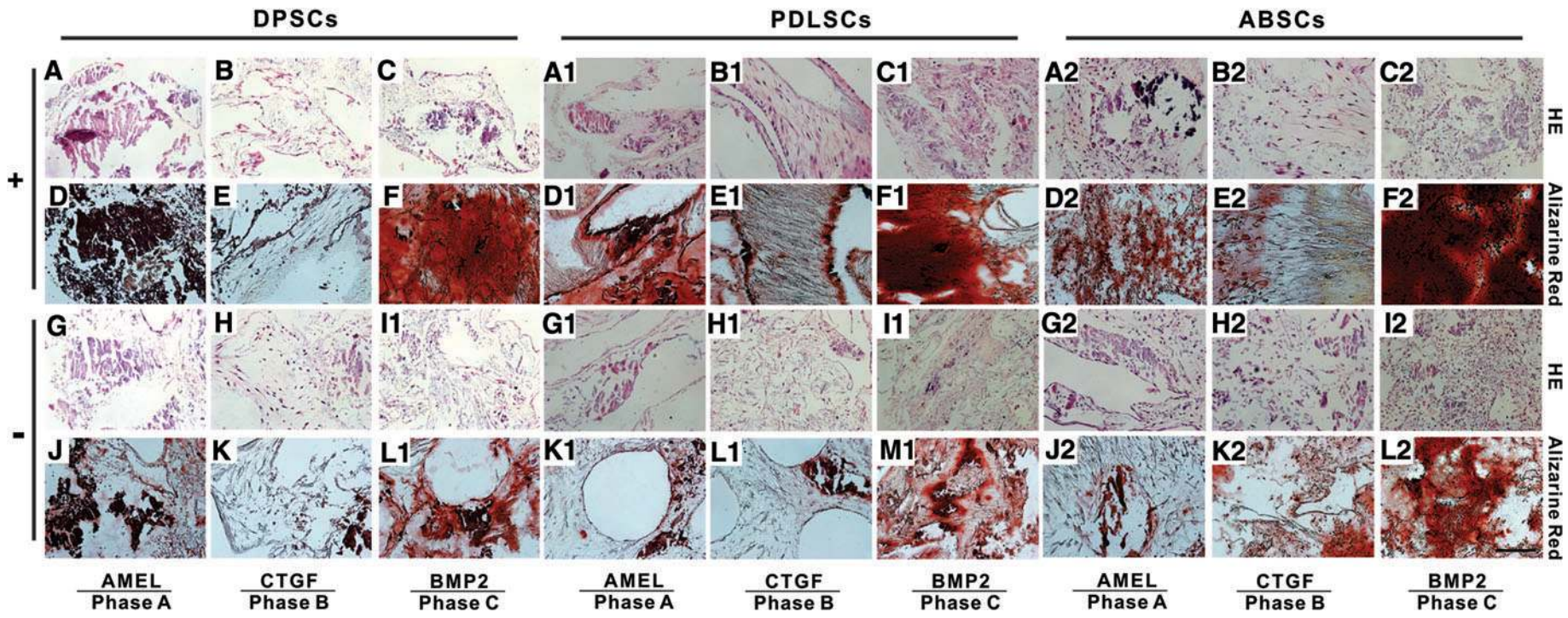

FIG. 2. Amelogenin, CTGF, and BMP2 induced region-specific tissue phenotype by three dental stem/progenitor cells *in vitro*. Dental pulp stem/progenitor cells (DPSCs), periodontal ligament stem/progenitor cells (PDLSCs), and alveolar bone stem/progenitor cells (ABSCs) were separately incubated with multiphase scaffolds, each region with different diameters. +: with protein encapsulated microspheres; −: empty microspheres without proteins. Amelogenin was delivered in Phase A, CTGF in Phase B, and BMP2 in Phase C. When cultured with DPSCs, mineralized tissue was formed in Phases A and C **(A, D, C, F)**, whereas nonmineralized fibrous matrix was formed in Phase B **(B, E)** upon stimulation with amelogenin, CTGF, and BMP2, respectively. Mineralized structure in Phase A was dense and polarized **(A, D)** in comparison to scattered mineral deposition in Phase C **(C, F)**. PDLSCs showed robust ability to form aligned collagen fiber-like structures in Phase B **(B1, E1)**, whereas ABSCs showed modest ability to form collagen fiber-like structures in Phase B **(B2, E2)**. However, both PDLSCs and ABSCs formed dense mineralized structure in Phase C **(C1, C2, F1, F2)**, although ABSCs only formed moderate mineral structures in Phase A **(A2, D2)**. PDLSCs showed scattered mineralization in Phase A (**A1**, **D1**). In control samples without amelogenin, CTGF, and BMP2 delivery, modest tissue phenotypes were formed **(G–L, G1–L1, G2–L2)**, although scaffold alone appeared to supportive mineralized tissue formation in **(L), (L1),** and **(L2)**. Scale bar = 100 μm. Color images available online at www.liebertpub.com/tea

previous methods.[47,48] Confocal microscopy was used to evaluate multiphase tissue formation in scaffolds without sectioning.

Data analysis and statistics

Upon confirmation of normal distribution, all quantitative data of control and treated groups were treated with one-way ANOVA and *post hoc* LSD tests at α level of 0.05.

Results

Multiphase tissue formation in cell-seeded scaffolds in vitro

Scaffolds with spatiotemporal delivery of bioactive cues formed distinctive multiphase tissues consisting of primitive PDL-like collagen fibers in Phase B that interfaced between mineralized bone-like tissues of Phases A and C that simulated dentin/cementum following 4-week *in vitro* incubation with DPSCs, PDLSCs, or ABSCs, respectively (Fig. 2). Remarkably, dense and polarized mineralized tissue was formed under amelogenin stimulation of DPSCs (Fig. 2A) in Phase A that was designed to simulate dentin/cementum formation. Spindle-shaped fibroblast-like cells in a nonmineralized matrix were present in CTGF-stimulated Phase B that was designed to simulate the PDL (Fig. 2B, E). Mineralized tissue was also formed in BMP2-stimulated Phase C that was seeded with DPSCs and designed for alveolar bone (Fig. 2C, F). Interestingly, scaffolds with empty μS also showed multiple tissues structures: mineralized tissues in Phases A and C (Fig. 2J, L) but nonmineralized tissue in Phase B (Fig. 2K), although mineralized tissue formation was not as robust as in amelogenin- or BMP2-delivered samples (Fig. 2D, F). Strikingly, collagen fiber-like structures were formed by PDLSCs under CTGF stimulation in Phase B, reminiscent of the native PDL (Fig. 2B1, 2E1). Dense mineralization was observed in Phase C with BMP2 stimulation of PDLSCs (Fig. 2C1, F1), but not as robust as in Phase A with amelogenin stimulation (Fig. 2D1). ABSCs yielded similar multitissue patterns with somewhat modest mineralization in Phase A (Fig. 2A2, D2) and robust mineralization in Phase C (Fig. 2C2, F2). Collagen fiber-like structures were formed by PDLSCs under CTGF stimulation in Phase B, reminiscent of the native PDL (Fig. 2B1, 2E1). Confocal microscopy demonstrated COL-I-rich nonmineralized soft tissue under CTGF stimulation in Phase B (Fig. 3B) that interfaced between $DSPP^+$ mineralized matrix in Phases A and C under amelogenin and BMP2 stimulations (Fig. 3A, C, respectively) and culture with DPSCs for 4 weeks. In contrasting, scaffolds with empty μS yielded scattered mineralization and modest COL-I (Fig. 3D–F).

Samples harvested at multiple time points (1, 2 and 3 weeks) demonstrated different mineralization patterns in Phase A than those in Phase C. In Phase A, polarized cell alignment was observed on scaffold's microstrand surface

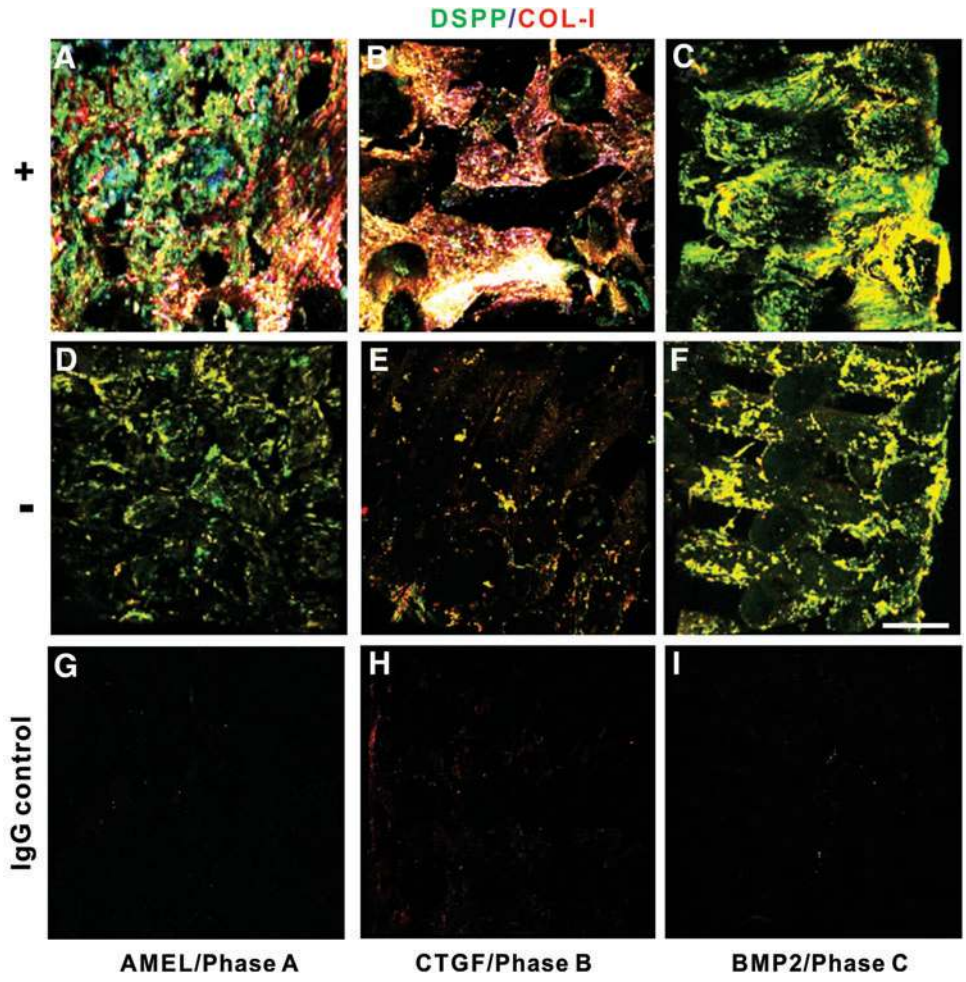

FIG. 3. Confocal microscopy of DPSC-seeded scaffolds. +: with protein encapsulated microspheres; −: empty microspheres without proteins. Following 4-week *in vitro* incubation, type I collagen (COL-I)-rich fibrous matrix in Phase B **(B)** interfaced between dentin sialophosphoprotein-positive ($DSPP^+$) mineralized regions in Phases A and C **(A, C)**. The right 1/3 of **(A)** shows integrated interface between COL-I-rich fibrous tissue and mineralized $DSPP^+$ matrix in Phase A. Modest $DSPP^+$ tissue was formed in control samples with empty microsphere **(D–F)**. Scale bar = 200 μm. Color images available online at www.liebertpub.com/tea

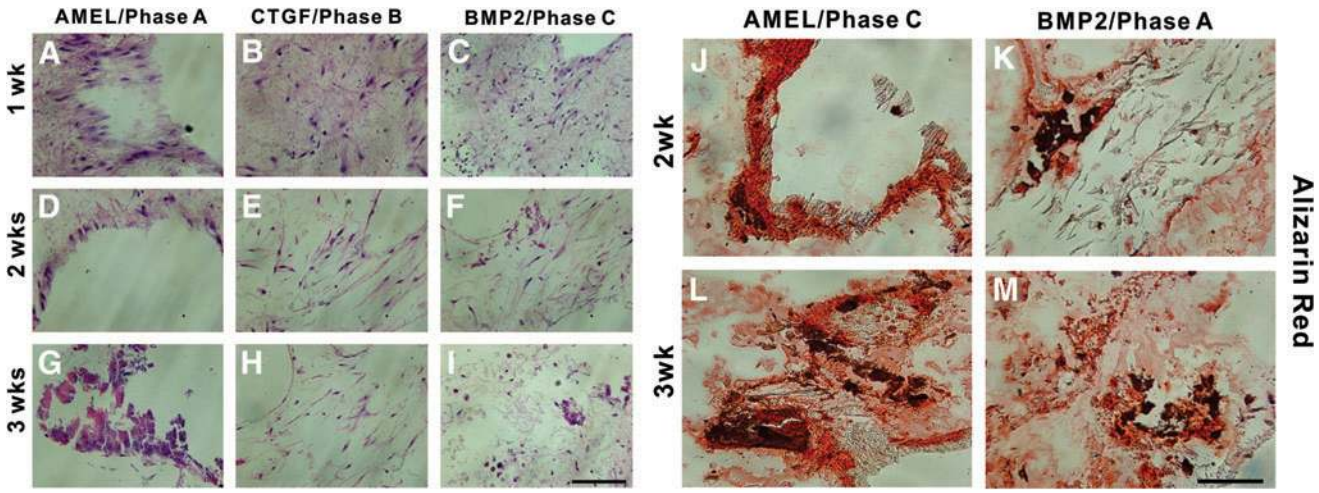

FIG. 4. Time line of mineralized tissue formation *in vitro* following 1, 2, and 3 weeks of culture of DPSCs. Amelogenin was delivered in Phase A, CTGF in Phase B, and BMP2 in Phase C. Mineral deposition in Phase C was relatively scattered from 1 to 3 weeks **(C, F, I, K, M)**. Contrastingly, polarized cell alignment was observed by 1 week, and mineralized matrix was deposited along with the aligned cells by 3 weeks to form polarized dense mineral structures in Phase A **(A, D, G, J, L)**. Phase B showed formation of spindle-shaped fibroblast-like cells **(B, E, H)**. Scale = 200 μm. Color images available online at www.liebertpub.com/tea

by 1 week and mineralized matrix was deposited along with the aligned cells by 3 weeks to form polarized dense mineral structures (Fig. 4A, D, H, K, M). In contrast, mineral deposition in Phase C was relatively scattered and isolated from 1 to 3 weeks (Fig. 4C, F, J, L, N). Spindle-shaped cells were observed as early as 2 weeks in Phase B (Fig. 4B, E, I).

Multiphase expression of mRNA markers

Real-time quantitative PCR showed that COL-I mRNA expression was significantly higher in Phase B than in Phases A and C (Fig. 5A). COL-I mRNA level was elevated by the delivery of bioactive cues (Fig. 5A). DSPP and CEMP1 mRNA expression was significantly higher in Phase A than in Phases B and C (Fig. 5B, D). BSP mRNA expression was significantly highly in Phase C than in Phases A and B (Fig. 5C). The expression of DSPP, CEMP1, and BSP mRNA was further enhanced in bioactive cues-delivered group than scaffolds with empty μS (Fig. 5B–D) ($n = 5$ per group; $p < 0.01$).

In vivo *generation of multiphase tissues mimicking periodontium complex*

After 4-week *in vivo* implantation, distinctive and yet integrated multiphase tissues were generated in DPSC-seeded scaffolds with spatiotemporal delivery of bioactive cues (Fig. 6). In Phase A, dense mineralized tissue was formed (Fig. 6A) and was positive to both AR (Fig. 6D) and DSPP (Fig. 6G). Unmineralized connective tissue was formed in

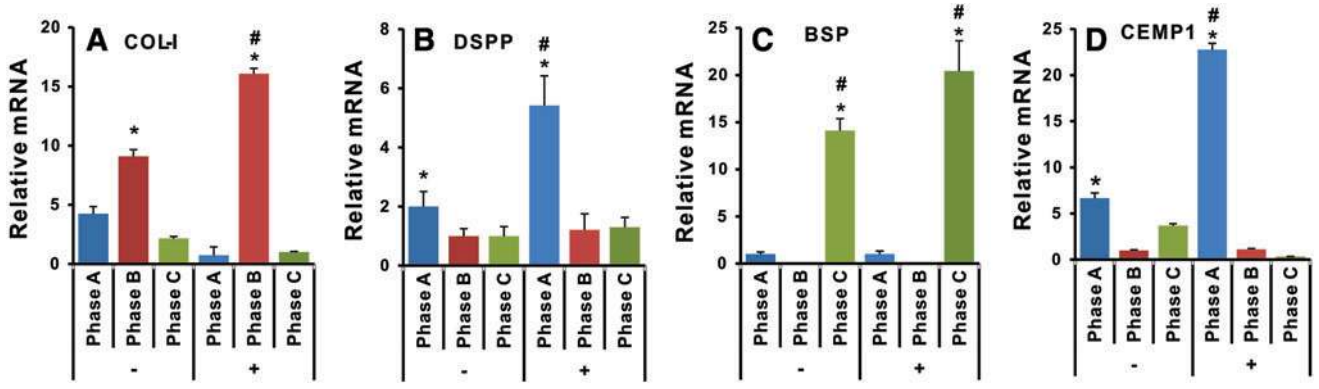

FIG. 5. mRNA expression of DPSCs cultured in multiphase scaffolds *in vitro*. +, with protein encapsulated microspheres; −, empty microspheres without proteins. Amelogenin was delivered in Phase A, CTGF in Phase B, and BMP2 in Phase C. COL-I mRNA was robustly expressed in Phase B and further elevated with CTGF stimulation **(A)**. DSPP and cementum matrix protein 1 (CEMP1) mRNA expression were significantly higher in Phase A than in Phases C and B and further elevated upon amelogenin stimulation **(B, D)**. Bone sialoprotein (BSP) mRNA was robustly expressed in Phase C and further elevated with BMP2 stimulation **(C)** ($n = 5$ per group; $^{*}p < 0.05$ for comparison among Phases A, B, and C; $^{\#}p < 0.05$ for comparison with or without protein stimulation). Color images available online at www.liebertpub.com/tea

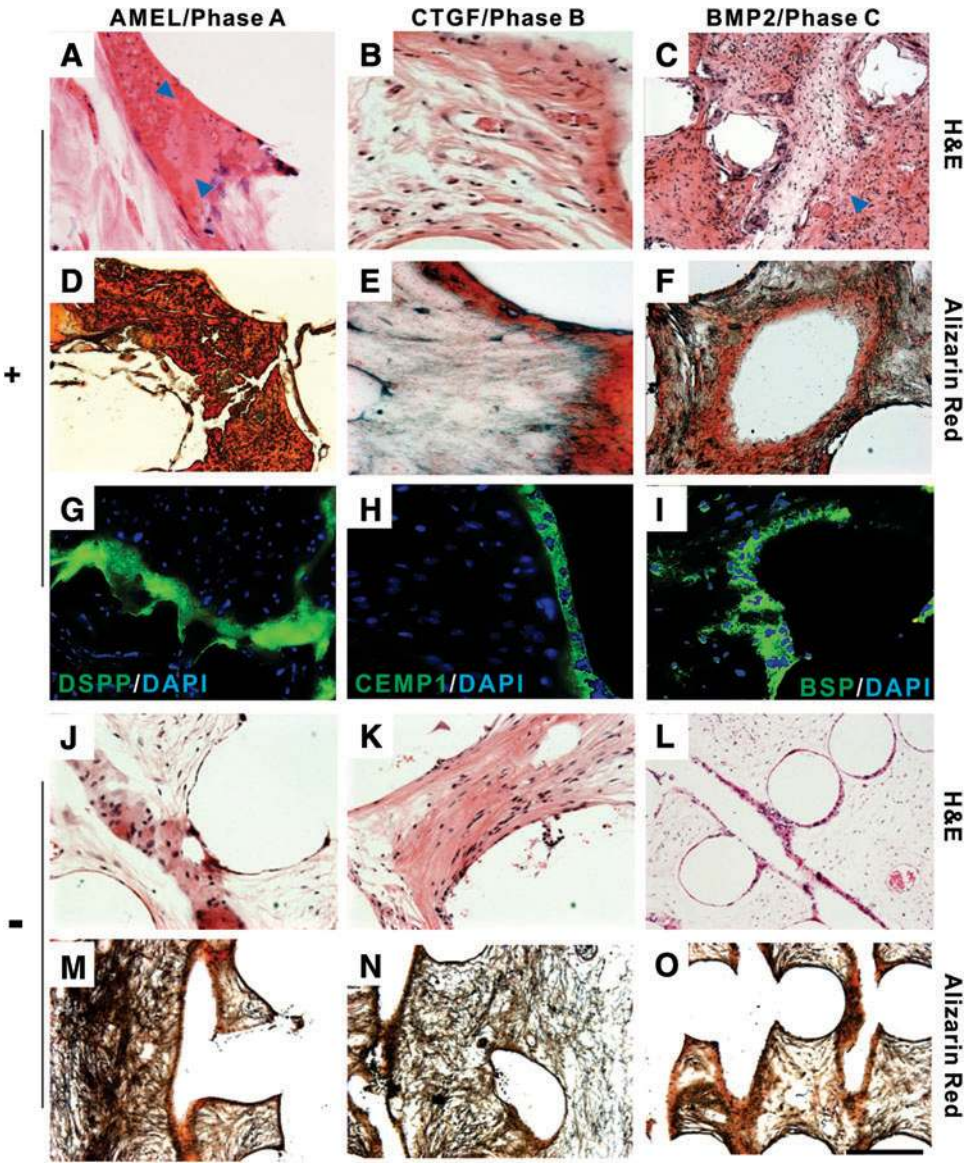

FIG. 6. Formation of collagen fibers inserting into mineralized dentin/cementum-like tissue and bone-like tissue *in vivo*. Upon 4-week *in vivo* implantation, the multiphase scaffolds with bioactive cues successfully led to the generation of mineralized tissues in Phases A and C **(A, C, D, F, G, I)** and aligned fibrous structure in Phase B **(B, E, H)**. Highly dense bulk DSPP$^+$ mineralized structure was observed in Phase A **(A, D, G)**, whereas BSP$^+$ alveolar bone-like mineralized tissue was formed in Phase C **(C, F, I)**. Impressively, aligned fibrous structure was inserted in CEMP1$^+$ mineralized matrix, resembling Sharpe's fibers, at Phases B–C interface **(B, E, H)**. Scaffolds with empty microspheres showed similar tendency with suboptimal tissue formation **(J–O)**. Scale bar = 200 μm for **(A, J,** and **M)**, and 100 μm for the others. S: scaffold. Arrows indicate mineralized regions. Color images available online at www.liebertpub.com/tea

Phase B not only with fibroblast-like cells and blood vessels (Fig. 6B) but also inserted into mineralized tissue that was positive to both AR (Fig. 6D) and CEMP (Fig. 6G), reminiscent of dental cementum. Phase C showed mineralized connective tissue (Fig. 6C), positive to AR (Fig. 6F) and also BSP (Fig. 6I), indicating mineralized bone-like tissue formation. Strikingly, Phase A seeded with DPSCs and stimulated with amelogenin (Fig. 6A, D, G) showed different tissue phenotype from that in Phase C containing the same population of DPSCs but stimulated with BMP2 (Fig. 6C, F, I), suggesting that amelogenin and BMP2 have differential effects on DPSCs. Immunofluorescence demonstrated that mineralized matrix in Phases A and C are positive for DSPP and BSP, respectively (Fig. 6G, I). Remarkably, aligned collagen fiber-like structures inserted into CEMP1$^+$ mineralized tissue, reminiscent of Sharpey's fibers at the interface between Phases B and C (Fig. 6B, E, H). Similar to our *in vitro* finding, scaffolds with empty μS showed similar tendency with suboptimal tissue formation (6D–F, J–L).

Discussion

Periodontium are complex and integrated anatomical structures with multiple region-specific tissue phenotypes, playing important roles in tooth function. The present findings suggest *de novo* formation of putative dentin/cementum-like structures and a PDL-like tissue interface both *in vitro* and *in vivo* by multiphase scaffolds with three distinctive microstructures and spatiotemporal delivery of BMP2, CTGF, and amelogenin. Multiple tissues consisting of BSP$^+$ bone-like tissue, Col-I$^+$ collagen fibers, and CEMP1$^+$/DSPP$^+$ dentin/cementum-like structures derive a single population of dental stem/progenitor cells *in vivo*. Previous periodontal tissues regeneration models have primarily adopted the approach of staggering multiple layers of biomaterials.[26,49–51] Although staggering of multiple biomaterial sheets is convenient for cell seeding, potential delamination of multiple layers is a concern. The present work takes advantage of our existing approach[33] of continuous 3D

printing to construct a seamless biomaterial scaffold and yet with different region-specific pore/channel sizes that are specifically designed for integrated regeneration of multiple periodontal tissues. The design of 100-μm transverse microchannels in Phase A is to serve as a module for cementum/dentin interface, preoptimized from our pilot study (Supplementary Fig. S2). The rationale for 600-μm transverse microchannels in Phase B is to simulate the width of the native PDL in the range of ~200 to 700 μm.[35] Furthermore, the design of 300-μm transverse microchannels in Phase C with a width of 2.25 mm for alveolar bone is to provide sufficient space in a pore size that is consistent with osteogenesis.[52] Cell seeding is convenient by hydrogel infusion in microchanneled scaffolds as shown in our present work. Our observation of Sharpey fiber-like structures inserting into $DSPP^+$ and $CEMP1^+$ mineralized cementum-like tissue on one side and BSP^+ bone-like tissue on the other side *in vivo* indicates the formation of a putative periodontium including putative dentin/cementum, PDL, and alveolar bone. This putative periodontium, in conjunction with $DSPP^+$ mineralized dentin-like tissue *in vivo*, arguably serves as a prototype for additional work for orthotopic regeneration of tooth root–periodontium complex. The pattern and size of microchannels/microstrands are readily adjustable while maintaining physical integration,[33,34,52] consequently leading to the generation of integrated multiple tissues.

As an extension of our previous experience in the regeneration of bone and fibrous defects *in vivo*,[31,33,34,36] we designed microchannels with biophysical parameters specifically for the regeneration of multitissue periodontium in the present study. A distinctive microarchitecture consists of interconnectivity and surface tomography in layer-deposited scaffolds and serves as pivotal cues for odontoblastic differentiation together with microchannel size. Microstructure with 100-μm microchannels in layer-deposited scaffolds appears to provide an appropriate biophysical configuration to the deposition of polarized dense mineralized structure, reminiscent of dentin. Our data showed that 100-μm channels in 3D-printed scaffolds are superior in promoting odontoblastic differentiation than other channel sizes tested (Supplementary Fig. S2). Channel sizes bigger than 100 μm (200 ~ 300 μm) failed to yield odontoblastic differentiation (data not shown). Although microstructure on native dentin surface consisting with 2–3 μm dentinal tubules is presumably appropriate to induce odontoblastic differentiation of DPSCs,[53] our data indicate that $DSPP^+$ tissue formation in 100-μm channels may allow putative odontoblasts to extend their processes and form multiple units of 2–3 μm dentinal tubules.

Dental stem/progenitor cells from various anatomical entities have been used for the regeneration of tooth and/or periodontal tissues. Cotransplantation of embryonic tooth germ cells in collagen gel in an extraction socket successfully leads to tooth morphogenesis, followed by eruption.[54,55] However, autologous embryonic tooth germ cells are not realistic for clinical applications.[13,54,55] Xenogenic or allogeneic embryonic tooth germ cells are not practical either due to ethical concerns, potential immunorejection and dismorphogenesis. The present findings show a potential of postnatal dental stem/progenitor cells, including DPSCs, PDLSCs, and ABSCs, for regenerating multiple periodontal tissues. Postnatal dental stem/progenitor cells, despite their inability to generate complete tooth organs, may retain the potency to differentiate into fibroblastic lineages[31] and into mineralized tissues that express dentin-like and bone-like markers, as shown in the present study. Some of dental stem/progenitor cells are present in tooth extraction sockets (e.g., PDLSCs and ABSCs) or can be readily isolated from dental tissues without undue trauma to the patient (e.g., PDLSCs and DPSCs). Host endogenous PDL cells and/or alveolar bone cells, including PDLSCs and ABSCs, can be recruited into scaffolds and instructed for regenerating periodontal tissues, as shown in our previous work.[9] Recruitment and directed differentiation of host endogenous cells may circumvent some of cell delivery-related translational hurdles.[33,56]

A limitation of the present *de novo* formation of putative periodontium complex upon ectopic implantation can be addressed by additional experiments to regenerate the periodontium orthotopically in a preclinical large animal model, as previously attempted for periodontal regeneration but without tooth roots.[57,58] Orthotopic regeneration in the same biochemical/physical environment as the native tissue that is to be replaced may further improve the quality and functionality of regenerating root and periodontal tissues. Together, multiphase periodontium tissues may regenerate by spatiotemporal delivery of multiple proteins and multiphase microstructure. A single stem/progenitor cell population appears to differentiate into putative dentin/cementum, PDL, and alveolar bone complex by scaffold's biophysical properties and specific bioactive cues. Apparently, it is speculated that optimal combination of microstructure and bioactive cues in consideration of a target cell type should be achieved for desirable periodontal tissues regeneration. Additional studies may further include investigations on signaling pathways involved in microstructure-/bioactive cues-induced cell differentiation for periodontium regeneration.

Acknowledgments

We thank Fen Guo for administrative and technical assistant. This work was funded by NIH/NIDCR grant RC2DE020767 and R01DE023112 to J.J.M.

Disclosure Statement

No competing financial interests exist.

References

1. Bai, Y., Matsuzaka, K., Hashimoto, S., Fukuyama, T., Wu, L., Miwa, T., *et al.* Cementum- and periodontal ligament-like tissue formation by dental follicle cell sheets co-cultured with Hertwig's epithelial root sheath cells. Bone **48,** 1417, 2011.
2. Li, Y., Jin, F., Du, Y., Ma, Z., Li, F., Wu, G., *et al.* Cementum and periodontal ligament-like tissue formation induced using bioengineered dentin. Tissue Eng Part A **14,** 1731, 2008.
3. Nanci, A., and Bosshardt, D.D. Structure of periodontal tissues in health and disease. Periodontol 2000 **40,** 11, 2006.
4. Amar, S., and Han, X. The impact of periodontal infection on systemic diseases. Med Sci Monit **9,** RA291, 2003.

5. Pihlstrom, B.L., Michalowicz, B.S., and Johnson, N.W. Periodontal diseases. Lancet **366,** 1809, 2005.
6. Kim, J., and Amar, S. Periodontal disease and systemic conditions: a bidirectional relationship. Odontology **94,** 10, 2006.
7. Oral Health in America. A Report of the Surgeon General. Rockville, MD: Department of Health and Human Services, U.S. Public Health Service.
8. Bae, C.H., Kim, T.H., Chu, J.Y., and Cho, E.S. New population of odontoblasts responsible for tooth root formation. Gene Expr Patterns **13,** 197, 2013.
9. Kim, K., Lee, C.H., Kim, B.K., and Mao, J.J. Anatomically shaped tooth and periodontal regeneration by cell homing. J Dent Res **89,** 842, 2010.
10. Kim, T.H., Bae, C.H., Lee, J.C., Ko, S.O., Yang, X., Jiang, R., *et al.* beta-catenin is required in odontoblasts for tooth root formation. J Dent Res **92,** 215, 2013.
11. Mantesso, A., and Sharpe, P. Dental stem cells for tooth regeneration and repair. Expert Opin Biol Ther **9,** 1143, 2009.
12. Mao, J.J., and Prockop, D.J. Stem cells in the face: tooth regeneration and beyond. Cell Stem Cell **11,** 291, 2012.
13. Modino, S.A., and Sharpe, P.T. Tissue engineering of teeth using adult stem cells. Arch Oral Biol **50,** 255, 2005.
14. Na, S., Zhang, H., Huang, F., Wang, W., Ding, Y., Li, D., *et al.* Regeneration of dental pulp/dentine complex with a three-dimensional and scaffold-free stem-cell sheet-derived pellet. J Tissue Eng Regen Med 2013 [Epub ahead of print]; DOI: 10.1002/term.1686.
15. Nait Lechguer, A., Kuchler-Bopp, S., Hu, B., Haikel, Y., and Lesot, H. Vascularization of engineered teeth. J Dent Res **87,** 1138, 2008.
16. Ohazama, A., Modino, S.A., Miletich, I., and Sharpe, P.T. Stem-cell-based tissue engineering of murine teeth. J Dent Res **83,** 518, 2004.
17. Sonoyama, W., Liu, Y., Fang, D., Yamaza, T., Seo, B.M., Zhang, C., *et al.* Mesenchymal stem cell-mediated functional tooth regeneration in swine. PLoS One **1,** e79, 2006.
18. Staels, S., De Coster, P., Vral, A., Temmerman, L., and De Pauw G. An experimental study on periodontal regeneration after subcutaneous transplantation of rat molar with and without cryopreservation: an *in vivo* study. Cryobiology **66,** 303, 2013.
19. Wei, F., Song, T., Ding, G., Xu, J., Liu, Y., Liu, D., *et al.* Functional tooth restoration by allogeneic mesenchymal stem cell-based bio-root regeneration in swine. Stem Cells Dev **22,** 1752, 2013.
20. Yelick, P.C., and Vacanti, J.P. Bioengineered teeth from tooth bud cells. Dent Clin North Am **50,** 191, 2006.
21. Seo, B.M., Miura, M., Gronthos, S., Bartold, P.M., Batouli, S., Brahim, J., *et al.* Investigation of multipotent postnatal stem cells from human periodontal ligament. Lancet **364,** 149, 2004.
22. Dangaria, S.J., Ito, Y., Yin, L., Valdre, G., Luan, X., and Diekwisch, T.G. Apatite microtopographies instruct signaling tapestries for progenitor-driven new attachment of teeth. Tissue Eng Part A **17,** 279, 2011.
23. Engler, A.J., Sen, S., Sweeney, H.L., and Discher, D.E. Matrix elasticity directs stem cell lineage specification. Cell **126,** 677, 2006.
24. Lee, C.H., Cook, J.L., Mendelson, A., Moioli, E.K., Yao, H., and Mao, J.J. Regeneration of articular surface of synovial joint by cell homing. Lancet **376,** 440, 2010.
25. Lee, C.H., Shin, H.J., Cho, I.H., Kang, Y.M., Kim, I.A., Park, K.D., *et al.* Nanofiber alignment and direction of mechanical strain affect the ECM production of human ACL fibroblast. Biomaterials **26,** 1261, 2005.
26. Park, C.H., Rios, H.F., Jin, Q., Sugai, J.V., Padial-Molina, M., Taut, A.D., *et al.* Tissue engineering bone-ligament complexes using fiber-guiding scaffolds. Biomaterials **33,** 137, 2012.
27. Williams, J.M., Adewunmi, A., Schek, R.M., Flanagan, C.L., Krebsbach, P.H., Feinberg, S.E., *et al.* Bone tissue engineering using polycaprolactone scaffolds fabricated via selective laser sintering. Biomaterials **26,** 4817, 2005.
28. Woodfield, T.B., Van Blitterswijk, C.A., De Wijn, J., Sims, T.J., Hollander, A.P., and Riesle, J. Polymer scaffolds fabricated with pore-size gradients as a model for studying the zonal organization within tissue-engineered cartilage constructs. Tissue Eng **11,** 1297, 2005.
29. Valles-Lluch, A., Novella-Maestre, E., Sancho-Tello, M., Pradas, M.M., Ferrer, G.G., and Batalla, C.C. Mimicking natural dentin using bioactive nanohybrid scaffolds for dentinal tissue engineering. Tissue Eng Part A **16,** 2783, 2010.
30. Viswanathan, H.L., Berry, J.E., Foster, B.L., Gibson, C.W., Li, Y., Kulkarni, A.B., *et al.* Amelogenin: a potential regulator of cementum-associated genes. J Periodontol **74,** 1423, 2003.
31. Lee, C.H., Shah, B., Moioli, E.K., and Mao, J.J. CTGF directs fibroblast differentiation from human mesenchymal stem/stromal cells and defines connective tissue healing in a rodent injury model. J Clin Invest **120,** 3340, 2010.
32. Chen, D., Zhao, M., and Mundy, G.R. Bone morphogenetic proteins. Growth Factors **22,** 233, 2004.
33. Lee, C.H., Cook, J.L., Mendelson, A., Moioli, E.K., Yao, H., and Mao, J.J. Regeneration of the articular surface of the rabbit synovial joint by cell homing: a proof of concept study. Lancet **376,** 440, 2010.
34. Lee, C.H., Marion, N.W., Hollister, S., and Mao, J.J. Tissue formation and vascularization in anatomically shaped human joint condyle ectopically *in vivo*. Tissue Eng Part A **15,** 3923, 2009.
35. Orban, B.J. Orban's Oral Histology and Embryology. Mosby, St. Louis, 1980.
36. Hong, L., and Mao, J.J. Tissue-engineered rabbit cranial suture from autologous fibroblasts and BMP2. J Dent Res **83,** 751, 2004.
37. Bansal, A.K., Shetty, D.C., Bindal, R., and Pathak, A. Amelogenin: a novel protein with diverse applications in genetic and molecular profiling. Journal of oral and maxillofacial pathology: JOMFP **16,** 395, 2012.
38. Moioli, E.K., Hong, L., Guardado, J., Clark, P.A., and Mao, J.J. Sustained release of TGFbeta3 from PLGA microspheres and its effect on early osteogenic differentiation of human mesenchymal stem cells. Tissue Eng **12,** 537, 2006.
39. Papagerakis, P., Berdal, A., Mesbah, M., Peuchmaur, M., Malaval, L., Nydegger, J., *et al.* Investigation of osteocalcin, osteonectin, and dentin sialophosphoprotein in developing human teeth. Bone **30,** 377, 2002.
40. Popowics, T., Foster, B.L., Swanson, E.C., Fong, H., and Somerman, M.J. Defining the roots of cementum formation. Cells Tissues Organs **181,** 248, 2005.
41. Nie, H., Lee, C.H., Tan, J., Lu, C., Mendelson, A., Chen, M., *et al.* Musculoskeletal tissue engineering by endogenous stem/progenitor cells. Cell Tissue Res **347,** 665, 2012.
42. Yang, R., Chen, M., Lee, C.H., Yoon, R., Lal, S., and Mao, J.J. Clones of ectopic stem cells in the regeneration of muscle defects *in vivo*. PLoS One **5,** e13547, 2010.

43. Yildirim, S., Fu, S.Y., Kim, K., Zhou, H., Lee, C.H., Li, A., *et al.* Tooth regeneration: a revolution in stomatology and evolution in regenerative medicine. Int J Oral Sci **3,** 107, 2011.
44. Alhadlaq, A., Elisseeff, J.H., Hong, L., Williams, C.G., Caplan, A.I., Sharma, B., *et al.* Adult stem cell driven genesis of human-shaped articular condyle. Ann Biomed Eng **32,** 911, 2004.
45. Marion, N.W., and Mao, J.J. Mesenchymal stem cells and tissue engineering. Methods Enzymol **420,** 339, 2006.
46. Yang, P.J., and Temenoff, J.S. Engineering orthopedic tissue interfaces. Tissue Eng Part B Rev **15,** 127, 2009.
47. Alhadlaq, A., and Mao, J.J. Tissue-engineered osteochondral constructs in the shape of an articular condyle. J Bone Joint Surg Am **87,** 936, 2005.
48. Sundaramurthy, S., and Mao, J.J. Modulation of endochondral development of the distal femoral condyle by mechanical loading. J Orthop Res **24,** 229, 2006.
49. Lu, H.H., Subramony, S.D., Boushell, M.K., and Zhang, X. Tissue engineering strategies for the regeneration of orthopedic interfaces. Ann Biomed Eng **38,** 2142, 2010.
50. Samavedi, S., Guelcher, S.A., Goldstein, A.S., and Whittington, A.R. Response of bone marrow stromal cells to graded co-electrospun scaffolds and its implications for engineering the ligament-bone interface. Biomaterials **33,** 7727, 2012.
51. Spalazzi, J.P., Dagher, E., Doty, S.B., Guo, X.E., Rodeo, S.A., and Lu, H.H. *In vivo* evaluation of a multiphased scaffold designed for orthopaedic interface tissue engineering and soft tissue-to-bone integration. J Biomed Mater Res A **86,** 1, 2008.
52. Hollister, S.J. Porous scaffold design for tissue engineering. Nat Mater **4,** 518, 2005.
53. Huang, G.T., Shagramanova, K., and Chan, S.W. Formation of odontoblast-like cells from cultured human dental pulp cells on dentin *in vitro*. J Endod **32,** 1066, 2006.
54. Ikeda, E., Morita, R., Nakao, K., Ishida, K., Nakamura, T., Takano-Yamamoto, T., *et al.* Fully functional bioengineered tooth replacement as an organ replacement therapy. Proc Natl Acad Sci U S A **106,** 13475, 2009.
55. Nakao, K., Morita, R., Saji, Y., Ishida, K., Tomita, Y., Ogawa, M., *et al.* The development of a bioengineered organ germ method. Nat Methods **4,** 227, 2007.
56. Mao, J., Stosich, M.S., Moioli, E., Lee, C.H., Fu, S., Bastian, B., *et al.* Facial reconstruction by biosurgery: cell transplantation vs. cell homing. Tissue Eng Part B Rev **16,** 257, 2010.
57. Carlo Reis, E.C., Borges, A.P., Araujo, M.V., Mendes, V.C., Guan, L., and Davies, J.E. Periodontal regeneration using a bilayered PLGA/calcium phosphate construct. Biomaterials **32,** 9244, 2011.
58. Emerton, K.B., Drapeau, S.J., Prasad, H., Rohrer, M., Roffe, P., Hopper, K., *et al.* Regeneration of periodontal tissues in non-human primates with rhGDF-5 and beta-tricalcium phosphate. J Dent Res **90,** 1416, 2011.

Address correspondence to:
Jeremy J. Mao, DDS, PhD
Center for Craniofacial Regeneration (CCR)
Columbia University Medical Center
630 W. 168 St.–PH7E—CDM
New York, NY 10032

E-mail: jmao@columbia.edu

Received: June 26, 2013
Accepted: November 25, 2013
Online Publication Date: February 4, 2014